Global Aromaticity in Neutral Porphyrin Nanobelts

Marco Vitek,[a,b] Jie-Ren Deng, [a] Harry L. Anderson,[a] Igor Rončević*[a]

[a] Marco Vitek, Dr. Jie-Ren Deng, Prof. Harry L. Anderson, Dr. Igor Rončević
Department of Chemistry, University of Oxford, Chemistry Research Laboratory, Oxford OX1 3TA, United Kingdom
E-mail: igor.roncevic@chem.ox.ac.uk

[b] Marco Vitek
Institute of Organic Chemistry and Biochemistry of the Czech Academy of Sciences
Flemingovo nám. 542/2, 160 00 Prague 6, Czechia

Supporting information for this article is given via a link at the end of the document.

Abstract: The ability of a ring-shaped molecule to sustain a global ring current, when placed in a magnetic field, indicates that its electronic wavefunction is coherently delocalized around its whole circumference. Large molecules that display global ring currents are attractive components for molecular electronic devices because it should be possible to control charge transport through these molecules using quantum interference. Here, we use theoretical methods to investigate how the global ring currents in molecular nanobelts built from edge-fused porphyrins evolve with increasing ring size. Our predictions were validated by using coupled clusters to construct a density functional approximation (denoted OX-B3LYP) that is specifically tailored to accurately describe these nanobelts. The results indicate that a global ring current persists in neutral belts consisting of up to about 22 porphyrin units, with Hückel circuits of 220 electrons (circumference 18.6 nm), which is surprising because global ring currents have not previously been reported in neutral macrocycles of this size.

The miniaturization of electronic circuits using conventional top-down fabrication has become limited by deleterious quantum effects, such as tunneling, which start to appear at the scale of a few nm.[2] Bottom-up fabrication with molecular electronic components offers a fascinating alternative, as well-designed single-molecule devices can exploit quantum effects instead of being limited by them.[3] Edge-fused porphyrin nanoribbons (Figure 1a) are excellent candidates for such devices as the electronic wavefunction is coherently delocalized over long ribbons of this type, resulting in exceptionally low energy gaps,[4] quantum interference,[5] and length-independent conductance.[6] In this work, we explore the electronic delocalization in edge-fused porphyrin nanobelts ***c*-P*N*** (where *N* is the number of porphyrin units, Figure 1b) computationally, to guide the selection of synthetic targets.

In molecular rings, a coherently delocalized electronic wavefunction causes the appearance of a global ring current under an externally applied magnetic field. This ring current produces shielding patterns that may be described using a particle-on-a-ring (POR) model. Hückel's rule states that systems with circuits of 4*n*+2 π-electrons (where *n* is an integer) sustain a diatropic current associated with aromaticity, while 4*n* π-systems sustain an anti-aromatic paratropic current.[7] As ring size increases, ring currents tend to become weaker due to symmetry-breaking and structural flexibility, which interrupt electronic delocalization.[8]

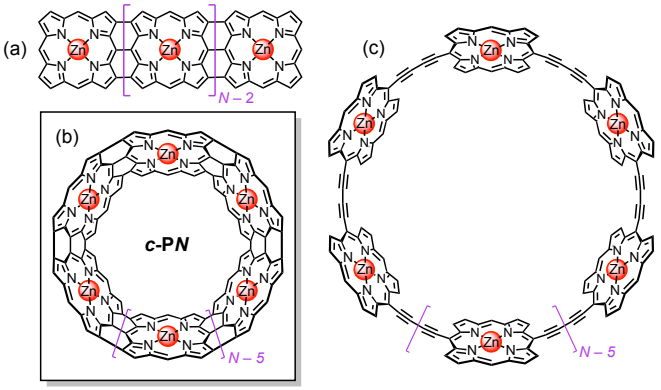

Figure 1. Porphyrin nanostructures. (a) Edge-fused nanoribbons. (b) Triply-linked nanobelts ***c*-P*N***, investigated in this work. (c) Singly-linked nanorings.

NMR spectroscopy has revealed substantial global ring currents in butadiyne- (Figure 1c) and ethyne-linked nanorings with circuits of up to 162 π-electrons (*n* = 40).[8-9] These singly-linked nanorings only show global ring currents in their charged states, where Coulombic repulsion promotes a more uniform charge distribution around the ring. In contrast, we demonstrate here that triply-linked ***c*-P*N*** nanobelts (Figure 1b) are expected to exhibit global ring currents even in the neutral state, due to the stronger coupling between the porphyrin subunits. Here, we address the question: What is the largest ***c*-P*N*** nanobelt that sustains a global ring current, in the neutral state? This work is part of a wider project exploring the frontier between molecular rings and top-down fabricated non-molecular nanorings that also exhibit persistent ring currents.[8]

While the experimental identification of global ring currents using NMR spectroscopy is often unambiguous, theoretical modelling is more challenging, particularly when using density functional theory (DFT) and nucleus-independent chemical shift (NICS) calculations.[10] This is not surprising, as the extent of symmetry breaking and electronic delocalization in conjugated systems is highly sensitive to the choice of method,[11] as first noted by Longuet-Higgins and Salem in 1959.[12] This is especially apparent in the case of hybrid DFT, which builds on pure Kohn-

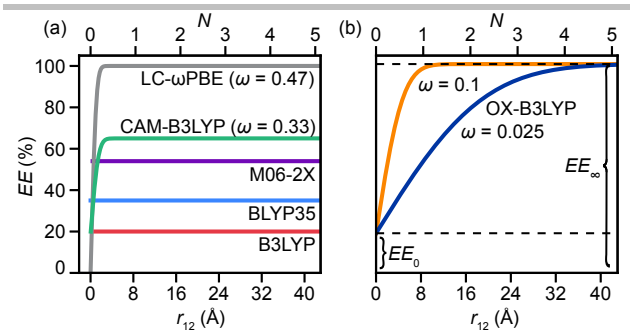

Figure 2. Variation of exact exchange (*EE*) with interelectronic distance (r_{12}) in (a) popular hybrid DFAs, and (b) the OX-B3LYP DFA, with two ω values (in units of a_0^{-1}) shown. *N* in the upper length scales indicates the number of edge-fused porphyrin units.

Sham DFT by including a proportion of exact exchange (EE) in the density functional. Adding EE reduces the self-interaction error, which is one of the main weaknesses of pure DFT, but adding too much EE causes too much localization by underestimating dynamic correlation, which pure DFT generally handles very well.[13]

The difficulty of striking the right balance between localization (too much EE) and delocalization (too little EE) can be illustrated by the case of the butadiyne-linked 6-porphyrin nanoring in its 6+ oxidation state (Figure 1c). For this system, B3LYP[14] (19% EE) overestimates the experimentally measured global ring current,[9b],16 M06-2X[15] (54%) underestimates it,[16] while BLYP35 (35%) reproduces the experimental results.[17] All of these DFAs have a constant proportion of EE (red, light blue, and purple in Figure 2a), which results in an incorrect description of the Coulomb interaction in the long-range limit and a poor description of charge transfer. Range-separated DFAs (e.g. LC-ωPBE,[18] gray in Figure 2a), in which the proportion of EE is dependent on the interelectronic distance r_{12}, remedy this issue,[19] but need three tunable parameters: EE_0 and EE_∞, which control the proportion of EE at the short- (r_{12} = 0) and long-range (r_{12} = ∞) limits, and ω (usually given in units of reciprocal Bohr radius, a_0^{-1}, with a_0 = 0.52 Å) , which controls the transition from EE_0 to EE_∞ (Figure 2b). In the case of the above-mentioned butadiyne-linked 6-porphyrin nanoring hexacation, the range separated functionals CAM-B3LYP[20] (green in Figure 2a) and a modified flavor of LC-ωPBE (ω = 0.1 a_0^{-1})[18] were both used to model its ring current, with good results.[16-17, 21]

At this point, the skeptical reader may rightly ask: If choosing a suitable DFA for modelling ring currents in nanorings for which experimental data are available is so difficult, what hope do we have of accurately predicting ring currents in ***c*-PN** nanobelts, which have yet to be synthesized? To answer this question, we recall that the equilibrium geometry of a conjugated system will be the result of a balance between the (distortive) π- and the (restorative) σ-electrons.[11c, 22] This balance will be highly dependent on the proportion of EE in hybrid DFT. Therefore, if we build a series of DFAs with different proportions of EE, the DFA providing the most accurate equilibrium geometry is likely to have the correct balance, and can be expected to give a reliable description of the electronic structure and ring current. We have recently shown that this hypothesis holds very well in case of [18]annulene, an archetypal conjugated system.[23] Using coupled clusters energies as reference (which are free from self-interaction error, but also include dynamic correlation), we identified BLYP45 (45% EE) as the optimal functional and found that it reproduces chemical shifts in both [18]annulene and its anions with a <1 ppm accuracy over a >30 ppm range. Similar approaches have been used successfully to identify appropriate DFAs for modelling interconversions between Hückel and Möbius topologies,[24] fullerene-based memristors,[25] and pericyclic reactions.[26] Here, we adopted the following general strategy (details in SI):

1. Optimize geometries of various ***c*-PN** nanobelts using several families of DFAs (PBE,[27] BLYP,[14] ωB97X[28]). Within each family, test many DFAs by changing the proportion of EE or EE_0, EE_∞, and ω.

2. Calculate the single-point energy for each optimized geometry of each ***c*-PN** using coupled clusters (or second-order perturbation theory, MP2, for larger belts). Identify the DFA that minimizes this energy, for each value of *N*. Keeping in mind that coupled clusters and MP2 calculations are sensitive to basis size, refine the DFA by correcting for basis set incompleteness.

3. Use the optimal DFA determined in (2.) to determine the NICS value at the center of the ring ($NICS(0)_{zz}$). This parameter provides a good probe of the ring current.

An alternative non-empirical approach for tuning a DFA for a specific system relies on making it compliant with Koopmans' theorem, which is usually accomplished by varying EE to match the negative HOMO energy and the vertical electron detachment energy of the neutral molecule.[29] Unfortunately, our attempts to construct a DFA using this approach failed (details in SI).

Following the strategy outlined above, we built OX-B3LYP (Optimized for eXtensively conjugated systems, dark blue in Figure 2b) as the optimal DFA for describing the ***c*-PN** nanobelts. At small r_{12}, OX-B3LYP (EE_0 = 19%) is virtually identical to B3LYP (*EE* = 19%), which is a suitable DFA for modelling the optical properties of edge-fused porphyrin nanoribbons (Figure 1a).[30] In the long-range limit, OX-B3LYP recovers the correct form of the Columbic decay (EE_∞ = 100%).

The most interesting feature of OX-B3LYP is the very low value of the range separation parameter (ω = 0.025 a_0^{-1}). This can be understood by noting that $1/\omega$ roughly corresponds to the distance at which electron-electron interactions are no longer screened (when EE_∞ = 100%). In general-purpose range-separated DFAs such the original LC-ωPBE (ω = 0.47 a_0^{-1}, grey in Figure 2a), $1/\omega$ is comparable to the length of a single bond ($1/\omega$ = 1.1 Å). In the LC-ωPBE variant suitable for singly-linked porphyrins (ω = 0.1 a_0^{-1}),[9b, 16-17, 21, 31] $1/\omega$ is on the order of a single porphyrin (5.3 Å), indicating that electrons are strongly delocalized within each porphyrin, but that inter-porphyrin interactions are unscreened. In OX-B3LYP (light blue in Figure 2b) screening persists up to several porphyrins in length (ω = 21.2 Å), reflecting strong inter-porphyrin coupling in ***c*-PN** nanobelts.

Each porphyrin unit in a ***c*-PN** nanobelt contributes 10 electrons to the Hückel count,[9b] so we expect even-numbered belts to sustain a paratropic ring current associated with anti-aromaticity (positive NICS inside the ring; red in Figure 3a) and the odd-numbered ones to display a diatropic current consistent with aromaticity (negative NICS inside the ring; blue in Figure 3b). Using OX-B3LYP we find that this is indeed the case, and predict that ***c*-P22** (circumference of 18.6 nm) as the largest nanobelt to show a ring-current-induced shift at the center of the ring larger than 1 ppm ($NICS(0)_{zz}$ of ±3 ppm corresponds to an isotropic shift

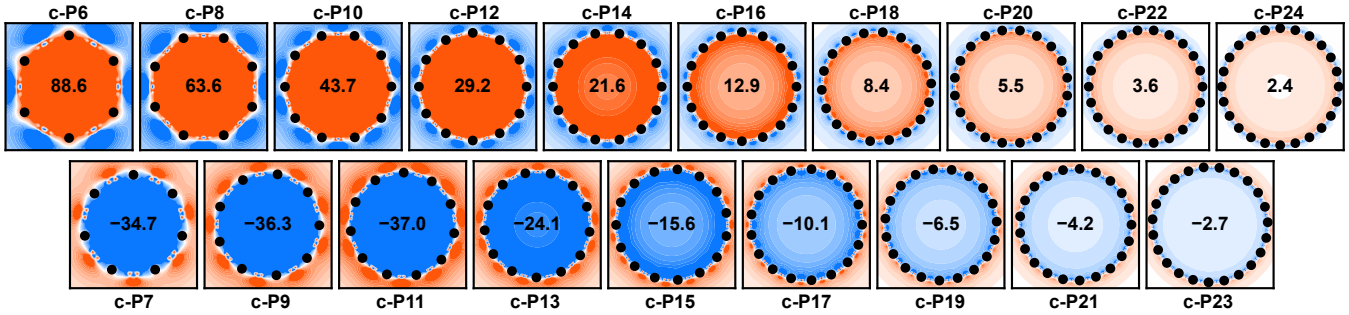

Figure 3. NICS(0)$_{zz}$ maps for ***c-PN*** nanobelts with N = 6–24, computed using OX-B3LYP. The NICS(0)$_{zz}$ value in the center of the ring is shown in bold.

of ±1 ppm, which is roughly the accuracy of DFT[32]; Figure 3). We also note that the best performing DFA with a constant proportion of EE (BLYP25) provides a very similar estimate (see SI).

We now shift our attention to evaluating the strain in molecular nanobelts. Template-directed synthesis, which is usually used to synthesize porphyrin nanorings,[33] starts conceptually from a porphyrin nanoribbon and then bends it into a ring (Figure 4a). This process is associated with a considerable increase in strain. We used OX-B3LYP and a hyperhomodesmotic[34] scheme (details in SI), to show that that the total strain in ***c-PN*** nanobelts decreases rapidly until about N > 12, then declines more gradually (Figure 4b,c). Combining these results with our NICS calculations, we can identify N = 16–18 nanobelts as the most attractive candidates for synthesis, offering relatively low strain energies and significant ring currents.

Another popular way to evaluate aromaticity is through aromatic stabilization energy (ASE), which is calculated as the difference in energy between an (anti-)aromatic cyclic system and a non-aromatic analogue, which may be linear or cross-conjugated.[35] Classic examples are cyclobutadiene and benzene, which have higher and lower energy, respectively, than their non-aromatic counterparts, corresponding to positive and negative ASE. OX-B3LYP calculations of ***c-PN*** nanobelts reveal similar behavior, with even-N belts (with 4n π-electrons) displaying a positive, and odd-N belts (with 4n+2 π-electrons) a negative ASE (Figure 4d). Here we calculate the ASE as the difference in energy between a particular ***c-PN*** and the smooth curve without the oscillation between aromatic and anti-aromatic species, thus avoiding the common problem of defining a non-aromatic reference system.[31] The energetic (ASE-based) criterion of aromaticity is somewhat more conservative than the magnetic (NICS-based) one, as the magnitude of ASE drops below 1 kJ/mol at N = 18 (Figure 4d), while a significant ring current persists up to at least N = 22 (Figure 4e).

Recognizing the importance of balancing the description of localization and delocalization in conjugated systems, here we used coupled clusters reference energies to build OX-B3LYP, a DFA specifically tuned for the description of edge-fused porphyrin nanobelts. OX-B3LYP predicts the presence of global ring currents in neutral belts with N up to 22, indicating global (anti-)aromaticity in molecular rings with a circumference of up to 18.6 nm. We expect that charged nanobelts will exhibit global ring currents at even larger sizes (e.g. N = 40), as indicated by our approximate calculations (see SI).

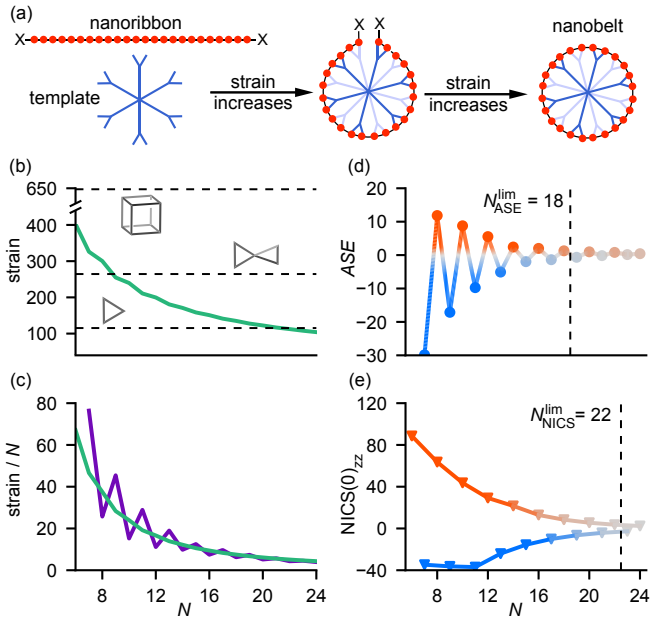

Figure 4. (a) Template-directed porphyrin nanoring synthesis. (b) Total strain energy (in kJ/mol) in ***c-PN*** nanobelts, compared to archetypal strained systems, cubane, bicyclopentane and cyclopropane (indicated by horizontal dashed lines).[1] (c) Strain energy per porphyrin (green) and strain release associated with increasing the belt size from N to N+1 (purple). (d) Aromatic stabilisation energy (ASE) per porphyrin and (e) NICS(0)zz at different belt sizes, with maximum ring sizes with |ASE| > 1 kJ/mol and |NICS(0)$_{zz}$| > 3 ppm denoted.

Supporting Information

The authors have cited additional references within the Supporting Information.

Acknowledgements

We thank the ERC (grant 885606, ARO-MAT, as well as grant 101095957, Q-SCALING) and UKRI (Horizon Europe Guarantee MSCA Postdoctoral Fellowship ElDelPath, EP/X030075/1) for funding. Computational resources were provided by the Cirrus UK National Tier-2 HPC Service at EPCC (http://www.cirrus.ac.uk) funded by the University of Edin-burgh and EPSRC (EP/P020267/1), as well as the Ministry of Education, Youth and Sports of the Czech Republic through the e-INFRA CZ (ID : 90140) and by the Oxford Advanced Research Computing (ARC) for computational resources (http://dx.doi.org/10.5281/zenodo.22558). M.V. acknowledges support from Charles University where he is enrolled as PhD. student and from the IMPRS for Quantum Dynamics and Control.

Keywords: ring current • aromaticity • density functional theory • porphyrin nanorings • molecular electronics

References

[1] K. B. Wiberg, *Angew. Chem. Int. Ed. Engl.* **1986**, *25*, 312-322.

[2] J. Shalf, *Phil. Trans. R. Soc. A* **2020**, *378*, 20190061.

[3] Z. Chen, I. M. Grace, S. L. Woltering, L. Chen, A. Gee, J. Baugh, G. A. D. Briggs, L. Bogani, J. A. Mol, C. J. Lambert, H. L. Anderson, J. O. Thomas, *Nat. Nanotechnol.* **2024**, doi: 10.1038/s41565-024-01633-1.

[4] A. Tsuda, A. Osuka, *Science* **2001**, *293*, 79-82.

[5] Z. Chen, J.-R. Deng, S. Hou, X. Bian, J. L. Swett, Q. Wu, J. Baugh, L. Bogani, G. A. D. Briggs, J. A. Mol, C. J. Lambert, H. L. Anderson, J. O. Thomas, *J. Am. Chem. Soc.* **2023**, *145*, 15265-15274.

[6] J.-R. Deng, M. T. González, H. Zhu, H. L. Anderson, E. Leary, *J. Am. Chem. Soc.* **2024**, *146*, 3651-3659.

[7] (a) R. Gershoni-Poranne, A. Stanger, *Chem. Soc. Rev.* **2015**, *44*, 6597-6615; (b) E. Steiner, P. W. Fowler, *Chem. Comm.* **2001**, 2220-2221.

[8] M. Jirásek, H. L. Anderson, M. D. Peeks, *Acc. Chem. Res.* **2021**, *54*, 3241-3251.

[9] (a) M. D. Peeks, M. Jirasek, T. D. W. Claridge, H. L. Anderson, *Angew. Chem. Int. Ed.* **2019**, *58*, 15717-15720; (b) M. Rickhaus, M. Jirasek, L. Tejerina, H. Gotfredsen, M. D. Peeks, R. Haver, H.-W. Jiang, T. D. W. Claridge, H. L. Anderson, *Nat. Chem.* **2020**, *12*, 236-241.

[10] D. Bradley, M. Jirásek, H. L. Anderson, M. D. Peeks, *Chem. Sci.* **2023**, *14*, 1762-1768.

[11] (a) S. Shaik, A. Shurki, D. Danovich, P. C. Hiberty, *Chem. Rev.* **2001**, *101*, 1501-1540; (b) K. Jug, P. C. Hiberty, S. Shaik, *Chem. Rev.* **2001**, *101*, 1477-1500; c. E. Heilbronner, *J. Chem. Educ.* **1989**, *66*, 471.

[12] H. C. Longuet-Higgins, L. Salem, *Phil. Trans. R. Soc. A* **1959**, *251*, 172-185.

[13] J. L. Bao, L. Gagliardi, D. G. Truhlar, *J. Phys. Chem. Lett.* **2018**, *9*, 2353-2358.

[14] A. D. Becke, *J. Chem. Phys.* **1993**, *98*, 5648-5652.

[15] Y. Zhao, D. G. Truhlar, *Theor. Chem. Acc.* **2008**, *120*, 215-241.

[16] I. Casademont-Reig, R. Guerrero-Avilés, E. Ramos-Cordoba, M. Torrent-Sucarrat, E. Matito, *Angew. Chem. Int. Ed.* **2021**, *60*, 24080-24088.

[17] J.-R. Deng, D. Bradley, M. Jirásek, H. L. Anderson, M. D. Peeks, *Angew. Chem. Int. Ed.* **2022**, *61*, e202201231.

[18] O. A. Vydrov, J. Heyd, A. V. Krukau, G. E. Scuseria, *J. Chem. Phys.* **2006**, *125*.

[19] G. Santra, R. Calinsky, J. M. L. Martin, *J. Phys. Chem. A* **2022**, *126*, 5492-5505.

[20] T. Yanai, D. P. Tew, N. C. Handy, *Chem. Phys. Lett.* **2004**, *393*, 51-57.

[21] I. Casademont-Reig, L. Soriano-Agueda, E. Ramos-Cordoba, M. Torrent-Sucarrat, E. Matito, *Angew. Chem. Int. Ed.* **2022**, *61*, e202206836.

[22] (a) G. Binsch, E. Heilbronner, J. N. Murrell, *Mol. Phys.* **1966**, *11*, 305-320; (b) P. W. Fowler, in *Advances in Quantum Chemistry, Vol. 44*, Academic Press, **2003**, pp. 219-237.

[23] W. Stawski, Y. Zhu, I. Rončević, Z. Wei, M. A. Petrukhina, H. L. Anderson, *Nat. Chem.* **2024**, doi: 0.1038/s41557-024-01469-1

[24] T. Woller, A. Banerjee, N. Sylvetsky, G. Santra, X. Deraet, F. De Proft, J. M. L. Martin, M. Alonso, *J. Phys. Chem. A* **2020**, *124*, 2380-2397.

[25] L. Tučková, A. Jaroš, C. Foroutan-Nejad, M. Straka, *Phys. Chem. Chem. Phys.* **2023**, *25*, 14245-14256.

[26] K. H. K. Park, N. Frank, F. Duarte, E. A. Anderson, *J. Am. Chem. Soc.* **2022**, *144*, 10017-10024.

[27] J. P. Perdew, K. Burke, M. Ernzerhof, *Phys. Rev. Lett.* **1996**, *77*, 3865-3868.

[28] Y.-S. Lin, G.-D. Li, S.-P. Mao, J.-D. Chai, *J. Chem. Theory Comput.* **2013**, *9*, 263-272.

[29] (a) L. Kronik, T. Stein, S. Refaely-Abramson, R. Baer, *J. Chem. Theory Comput.* **2012**, *8*, 1515-1531; (b) A. Karolewski, L. Kronik, S. Kümmel, *J. Chem. Phys.* **2013**, *138*, 204115; (c) D. Manna, J. Blumberger, J. M. L. Martin, L. Kronik, *Mol. Phys.* **2018**, *116*, 2497-2505.

[30] R. V. Belosludov, D. E. Nevonen, V. N. Nemykin, *J. Phys. Chem. A* **2021**, *125*, 2480-2491.

[31] M. Jirásek, M. Rickhaus, L. Tejerina, H. L. Anderson, *J. Am. Chem. Soc.* **2021**, *143*, 2403-2412.

[32] (a) G. L. Stoychev, A. A. Auer, R. Izsák, F. Neese, *J. Chem. Theory Comput.* **2018**, *14*, 619-637; (b) G. L. Stoychev, A. A. Auer, F. Neese, *J. Chem. Theory Comput.* **2018**, *14*, 4756-4771.

[33] (a) M. C. O'Sullivan, J. K. Sprafke, D. V. Kondratuk, C. Rinfray, T. D. W. Claridge, A. Saywell, M. O. Blunt, J. N. O'Shea, P. H. Beton, M. Malfois, H. L. Anderson, *Nature* **2011**, *469*, 72-75; (b) M. Hoffmann, C. J. Wilson, B. Odell, H. L. Anderson, *Angew. Chem. Int. Ed.* **2007**, *46*, 3122-3125; (c) H. Gotfredsen, J.-R. Deng, J. M. Van Raden, M. Righetto, J. Hergenhahn, M. Clarke, A. Bellamy-Carter, J. Hart, J. O'Shea, T. D. W. Claridge, F. Duarte, A. Saywell, L. M. Herz, H. L. Anderson, *Nat. Chem.* **2022**, *14*, 1436-1442.

[34] S. E. Wheeler, K. N. Houk, P. v. R. Schleyer, W. D. Allen, *J. Am. Chem. Soc.* **2009**, *131*, 2547-2560.

[35] G. Merino, M. Solà, I. Fernández, C. Foroutan-Nejad, P. Lazzeretti, G. Frenking, H. L. Anderson, D. Sundholm, F. P. Cossío, M. A. Petrukhina, J. Wu, J. I. Wu, A. Restrepo, *Chem. Sci.* **2023**.